JOURNAL OF MECHANICS OF CONTINUA AND MATHEMATICAL SCIENCES
www.journalimcms.org

ISSN (Online) : 2454 -7190 Vol.-15, No.-8, August (2020) pp 136-150 ISSN (Print) 0973-8975

A SCIENTIFIC APPROACH TO CONTROL THE SPEED DEVIATION OF DUAL REGULATED LOW-HEAD HYDRO POWER PLANT CONNECTED TO SINGLE MACHINE INFINITE BUS

Nagendrababu Mahapatruni[1], Velangini Sarat P.[2], Suresh Mallapu[3], Durga Syamprasad K.[4]

[1]Associate Professor, Department of Mechanical Engineering, Vignan's Institute of Engineering For Women, Visakhapatnam, Andhra Pradesh - 46, India

[2.3,4]Assistant Professor, Department of Electrical & Electronics Engineering, Vignan's Institute of Engineering For Women, Visakhapatnam, Andhra Pradesh - 46, India

[1]nagyie@ymail.com, [2]sarath.pilla283@gmail.com, [3]mlpsuresh@gmail.com, [4]kdurgasyam@gmail.com

Corresponding Author: Nagendrababu Mahapatruni

https://doi.org/10.26782/jmcms.2020.08.00013

(Received: June 9, 2020; Accepted: July 29, 2020)

Abstract

Analysis of single machine infinite bus system is made by considering single Kaplan turbine-generator with exciter and governor for the small-signal stability. In this research paper a scientific approach was adopted to minimize the settling time along with the stability of the given power system. Kaplan turbine generators were predominantly implemented in hydroelectric power plants with lower heads. However, dual regulation of such turbines in the plants are renowned in the current research trends. The dual regulation of hydro-turbine is incorporated through the operation of both wicket gate and runner blade position. In a worldwide scenario Kaplan turbine-generators play a vital role in power and energy generation. Whereas the life of these generator gates or runner blades depends on speed deviations. In this context, a PID controller has been designed for the extended single machine infinite bus system to improve the speed deviation. The results of the extended single machine infinite bus system are compared with and without PID controller for the enhancement of speed deviation.

Keywords : Power System, Extended SMIB, Governor, Speed deviation, PID controller.

I. Introduction

Electrical power systems are one of the complex constituents required for the generation, transmission along with large scale distribution of Electrical Energy

through any power or energy source. Such power systems should be capable of periodical adaptability to variable load demands corresponding to active and reactive power. Complex power system stability will be the state of operating equilibrium at normal operating conditions. (Chan & Aung, 2020) Synchronous machines in such power systems will have huge significance and wide range of applications in hydro prime movers such as turbines. In the emerging researches in power systems stability, the major challenge is in adequate damping of the corresponding system oscillations. Hence, in analyzing the stability of such power systems signal, a linearized illustration model was preferred to illustrate the required power system and its components. (Czeslaw Banka, 2017) The illustrations itself gives the state space representation with various operational inputs and outputs along with the internal behavior of the system. Transfer functions are one of prominent representations which illustrates the behavior of the input and output while a state-space illustration represents the system along with the transfer function along with its defined characteristics. (Ghosh, Das, & Sanyal, 2019) The context to the current research with the application state-space representation will give the complete details of the power system that can be significantly applied to the analysis of Multi-Variable MIMO systems which are ideal for optimized speeds versus toque characteristics. Present research is on use of pressure signal for speed control of hydro generator. Presently SMIB is extended to dual regulation of low- head hydro power plant with wicket gate opening and runner blade position for controlling the water pressure. The results of extended single machine infinite bus system are compared with and without PID controller for speed deviations. (Machowski, Bialek, & Bumby, 2020)

II. Mathematical Modeling of Extended Smib

Considering a single machine system neglecting damper windings both in the d and q axes. By neglecting the armature resistance of the machine, the excitation system is represented by a single time constant system is shown in Fig.1. (Bux, Xiao, Hussain, & Wang, 2019) The linearized model of SMIB is derived as follows:

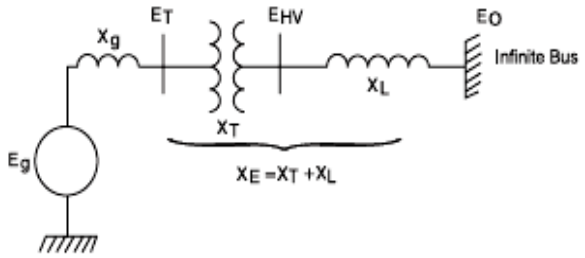

Fig. 1: A Single machine system

The linearized model of SMIB is derived as follows:

The algebraic equations of the stator are

$$E'_q + x'_d i_d = v_q \tag{1}$$

$$-x_q i_q = v_d \tag{2}$$

The complex terminal voltage can be expressed as

$$v_Q + jv_D = (v_q + jv_d)e^{j\delta} = (i_q + ji_d)(R_e + jx_e)e^{j\delta} + E_b\angle 0$$

$$(v_q + jv_d) = (i_q + ji_d)(R_e + jx_e) + E_b e^{-j\delta} \tag{3}$$

From equations. (1), (2) and (3) the expressions for i_d and i_q are

$$i_d = \frac{1}{A}\left[R_e E_b \sin\delta + (x_q + x_e)(E_b\cos\delta - E'_q)\right] \tag{4}$$

$$i_q = \frac{1}{A}\left[(x'_d + x_e)E_b\sin\delta - R_e(E_b\cos\delta - E'_q)\right] \tag{5}$$

Where,

$$A = (x'_d + x_e)(x_q + x_e) + R_e^2 \tag{6}$$

Linearizing Equations. (4) and (5) we get

$$\Delta i_d = C_1\Delta\delta + C_2\Delta E'_q \tag{7}$$

$$\Delta i_q = C_3\Delta\delta + C_4\Delta E'_q \tag{8}$$

Where,

$$C_1 = \frac{1}{A}\left[R_e E_b\cos\delta_o - (x_q + x_e)E_b\sin\delta_o\right]$$

$$C_2 = -\frac{1}{A}(x_q + x_e)$$

$$C_3 = \frac{1}{A}\left[(x'_d + x_e)E_b\cos\delta_o + R_e E_b\sin\delta_o\right]$$

$$C_4 = \frac{R_e}{A}$$

Linearizing Equations. (1) and (2) , and substituting from Equations. (7) and (8), we get,

$$\Delta v_q = x'_d C_1\Delta\delta + (1 + x'_d C_2)\Delta E'_q \text{ (9) } \Delta v_d = -x_q C_3\Delta\delta - x_q C_4\Delta E'_q \tag{9}$$

The subscript ‘o’ indicates operating value of the variable.

Rotor Mechanical Equations and Torque Angle Loop:

The rotor mechanical equations are

$$\frac{d\delta}{dt} = \omega_0(S_m - S_{mo}) \tag{10}$$

$$2H\frac{dS_m}{dt} = -DS_m + T_m - T_e \tag{11}$$

$$T_e = E'_q i_q - (x_q - x'_d)i_d i_q \tag{12}$$

Linearizing Eq. (13) we get

$$\Delta T_e = \left[E'_{qo} - (x_q - x'_d)i_{do}\right]\Delta i_q + i_{qo}\Delta E'_q - (x_q - x'_d)i_{qo}\Delta i_d \quad (13)$$

Substituting Equations. (7) and (8) in Eq. (14), we can express ΔT_e as

$$\Delta T_e = K_1\Delta\delta + K_2\Delta E'_q \quad (14)$$

Where,

$$K_1 = E_{qo}C_3 - (x_q - x'_d)i_{qo}C_1 \quad (15)$$

$$K_2 = E_{qo}C_4 + i_{qo} - (x_q - x'_d)i_{qo}C_2 \quad (16)$$

$$E_{qo} = E'_{qo} - (x_q - x'_d)i_{do} \quad (17)$$

Liberalizing Eqns. (11) and (12) and applying Laplace transform, we get

$$\Delta\delta = \frac{\omega_0}{s}\Delta S_m = \frac{\omega_0}{s}\Delta\bar{\omega} \quad (18)$$

$$\Delta S_m = \frac{1}{2Ms}[\Delta T_m - \Delta T_e - D\Delta S_m] \quad (19)$$

The combined Equations. (15), (19) and Eq. (20) represent a block diagram shown in Fig.2. This represents the torque-angle loop of the synchronous machine.

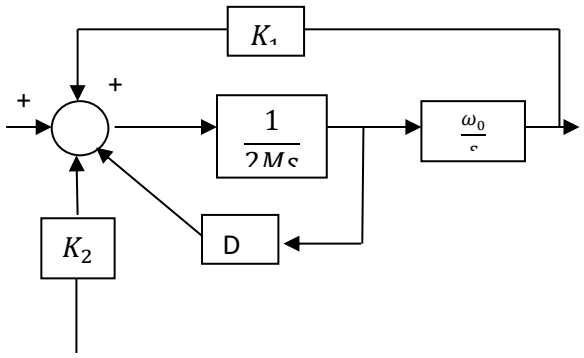

Fig. 2: Block diagram of Torque angle loop

Representation of Flux Decay:

The equation for the field winding can be expressed as

$$T'_{do}\frac{dE'_q}{dt} = E_{fd} - E'_q + (x_d - x'_d)i_d \quad (20)$$

Linearizing Eq. (21) and substituting from Eq. (7) we have

$$T'_{do}\frac{d\Delta E'_q}{dt} = \Delta E_{fd} - \Delta E'_q + (x_d - x'_d)(C_1\Delta\delta + C_2\Delta E'_q) \quad (21)$$

Taking Laplace transform of above equation we get,

$$(1 + sT'_{do}K_3)\Delta E'_q = K_3\Delta E_{fd} - K_3K_4\Delta\delta \quad (22)$$

Where,

$$K_3 = \frac{1}{[1-(x_d - x'_d)C_2]} \tag{23}$$

$$K_4 = -(x_d - x'_d)C_1 \tag{24}$$

The equation (23) is represented in block diagram which is the representation of flux decay is shown in Fig.3.

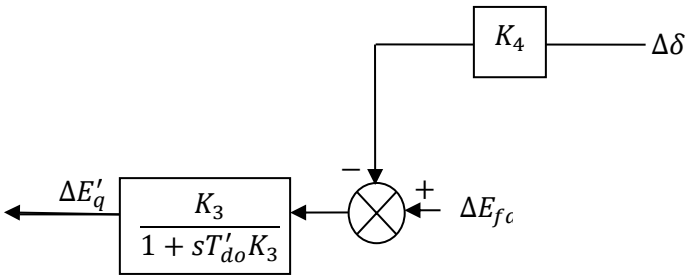

Fig. 3: Block diagram of Flux decay

Representation of Excitation System:

The block diagram of the excitation system is shown in Fig 2.4. The linearized equations involved in the analysis are described below and the terminal voltage ΔV_t can be expressed as

$$\Delta V_t = \frac{v_{do}}{V_{to}}\Delta v_d + \frac{v_{qo}}{V_{to}}\Delta v_q \tag{25}$$

Substituting from Equations. (2.12) and (2.13) in (2.31), we get

$$\Delta V_t = K_5\Delta\delta + K_6\Delta E'_q \tag{26}$$

Where,

$$K_5 = -\left(\frac{v_{do}}{V_{to}}\right)x_q C_3 + \left(\frac{v_{qo}}{V_{to}}\right)x'_d C_1 \tag{27}$$

$$K_6 = -\left(\frac{v_{do}}{V_{to}}\right)x_q C_4 + \left(\frac{v_{qo}}{V_{to}}\right)(1 + x'_d C_2) \tag{28}$$

Using the equation (27) the block diagram of the excitation system is obtained which is shown below in fig. 2.4.

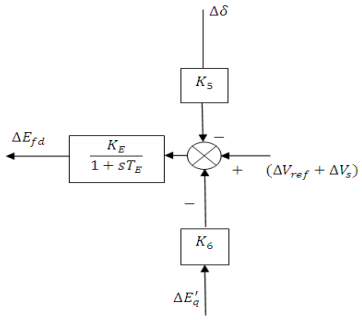

Fig. 4: Block diagram of Excitation loop

Representation of Turbine Flow Control:

The water flow through the penstock was modelled by considering the inelastic water column effect. Hence, the stiff water hammer equation can be given as

$$\frac{dh}{dt} = -T_w \frac{dw}{dt} \tag{29}$$

The turbine flow "q" and the torque "m" in case of a Kaplan turbine are non-linear functions of head "h", wicket gate opening "z", machine speed w and runner blade position θ. For a given reference operating point, the partial derivative relationship between these variables is given as

$$q = \frac{\delta q}{\delta h} h + \frac{\delta q}{\delta z} z + \frac{\delta q}{\delta w} w + \frac{\delta q}{\delta \theta} \theta \tag{30}$$

$$= T_1 h + T_2 z + T_3 w + T_4 \theta$$

$$m = \frac{\delta m}{\delta h} h + \frac{\delta m}{\delta z} z + \frac{\delta m}{\delta w} w + \frac{\delta m}{\delta \theta} \theta \tag{31}$$

$$= T_5 h + T_6 z + T_7 w + T_8 \theta \; ;$$

$$\frac{dq}{dt} = \frac{1}{T_W T_1} [T_3 w + T_2 z - q + T_4 \theta] \tag{32}$$

The operation of Kaplan turbine involves control of the wicket gate and the runner blade position in order to regulate the water flow to the hydro-turbine. The corresponding servomotor equations are described as

$$\frac{dz}{dt} = (U_{gov} - z)/T_{gv} \tag{33}$$

$$\frac{d\theta}{dt} = (U_{gov} - \theta)/T_r$$

Where T_{gv} and T_{rb} are wicket gate and runner blade servomotor constants respectively. The third order synchronous generator model is described by the following set of deferential and algebraic Equations:

$$T_a\frac{dw}{dt} = m - m_l - Dw \quad (34)$$

$$\frac{de'_q}{dt} = \frac{1}{T'_{d0}}[E_{FD} - \frac{1}{K3}\ e'_q - K_4\delta_l] \quad (35)$$

$$m_l = K_1\delta_l + K_2e'_q$$

Expressing the exciter equations are as follows:

$$\frac{dE_{FD}}{dt} = \frac{1}{T_E}[V_a - K_EE_{FD}] \quad (36)$$

$$\frac{dV_a}{dt} = \frac{1}{T_A}[K_A V_{ref} + K_A u_{ex} - K_A V_t - K_A V_f - V_a] \quad (37)$$

$$V_t = K_5\ \delta_l + K_6 \quad (38)$$

$$\frac{dv_f}{dt} = \frac{1}{T_F}[\frac{K_FK_E}{T_FT_E}\ E_{FD} + \frac{K_F}{T_E}\ V_a - V_f] \quad (39)$$

The block diagram representation for turbine flow control is shown in fig.2.5, block diagram representation for runner blade position is shown in fig.2.6 and the block diagram representation for wicket gate opening is shown in above figure.

The dynamic characteristics of the extended SMIB system are expressed in terms of constants K_1 to K_9. The constants K_7, K_8 and K_9 are due to head h, wicket gate opening z, machine speed w and runner blade position θ and they are,

$$K_7 = T_7 - (T_3T_5)T_1 \quad (40)$$

$$K_8 = T_6 - (T_5T_2)/T_1 \quad (41)$$

$$K_8 = T_8 - (T_5T_4)/T_1 \quad (42)$$

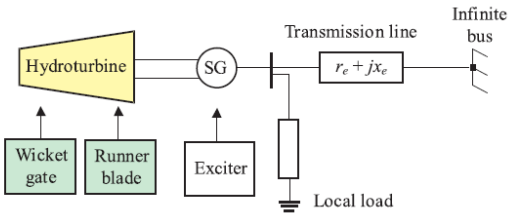

Fig. 5: Block diagram of EXTENDED SMIB

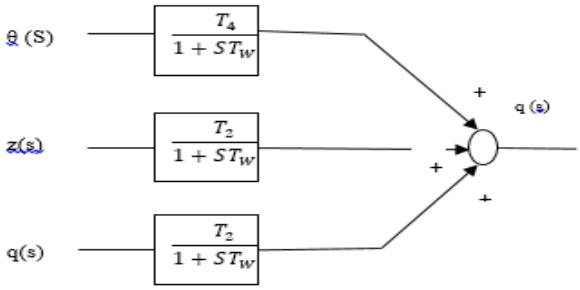

Fig. 6: Turbine flow control q(s)

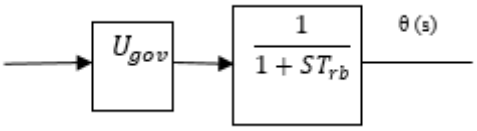

Fig. 7: Runner blade position θ (s)

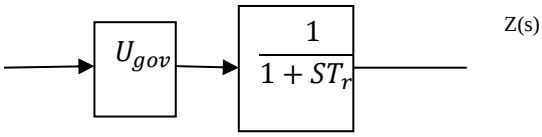

Fig. 8: Wicket gate opening z(s)

Where U_{gov} , U_{ex} are two input quantities

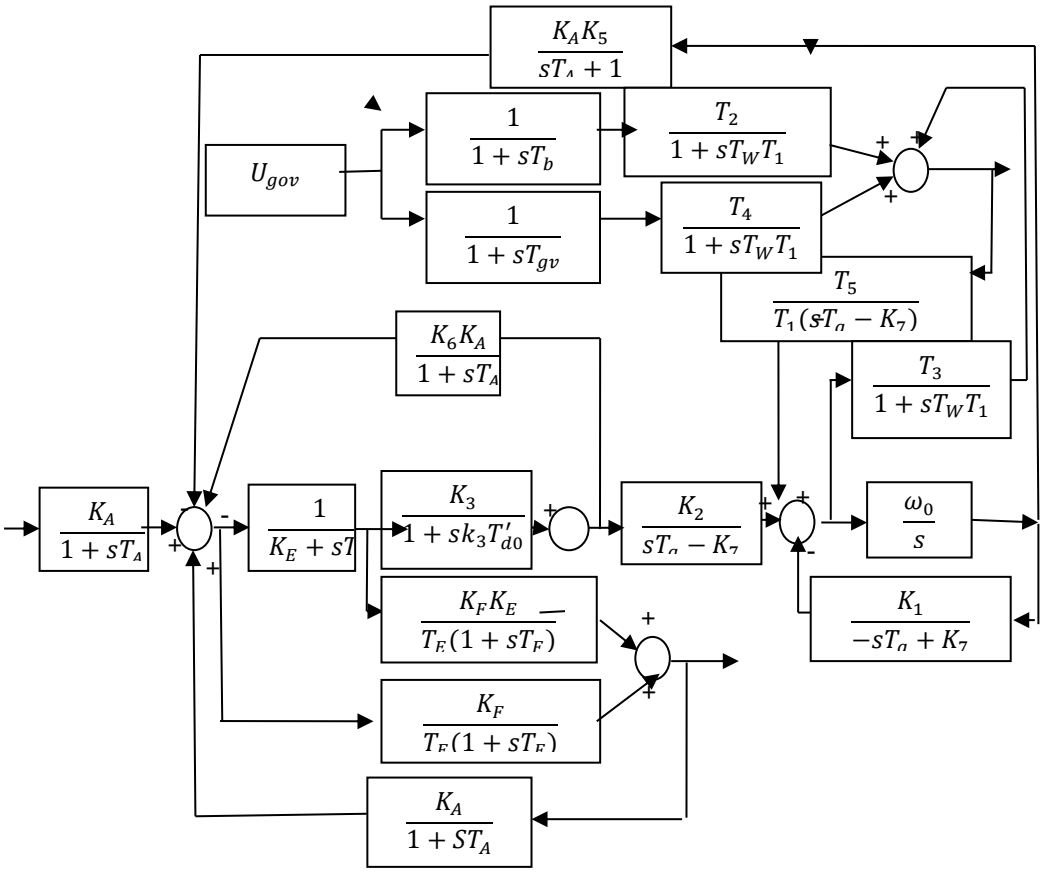

Fig. 9: Over all block diagram of extended SMIB

III. Controller

A PID (proportional–integral–derivative) controller was prescribed based on its damping controller along with the tuned fixed-gain parameters. A detailed illustration of the PID controlled was explained below.

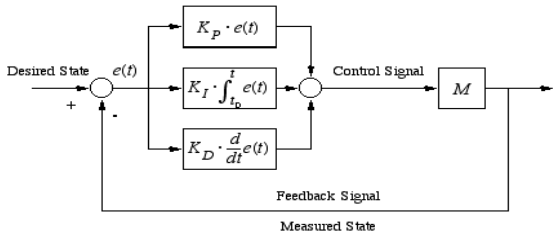

Fig. 10: Block diagram of PID Controller

A PID controller intends to rectify the error between a measured process variable and a desired set point by evaluating and then executing a necessary corrective action that can rectify the process in accordance with system stability. The PID controller evaluation/calculation (algorithm) consists 3 independent parameters; the Proportional, the Integral and the Derivative values. The Proportional value were used to determine the reaction to the speed deviation, the Integral value was used to determine the reaction based on the cumulative sum of recent errors, and the Derivative value was used to determine the reaction based on the rate of the variability of the error.

IV. Simulation Result

Simulations are done by using MATLAB Simulink. The graph drawn between speed deviation (y-axis) and time x-axis).

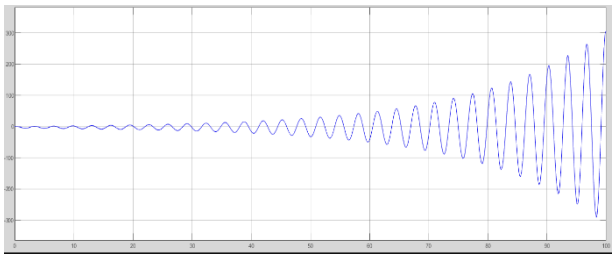

Fig. 11: speed deviation with respect to time for SMIB

As we can see in the above figure that the speed deviation signal is completely unstable and it leads to power system failure.

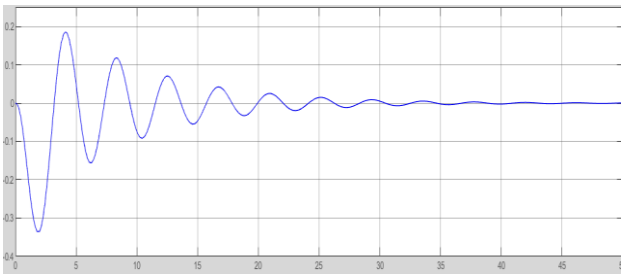

Fig. 12: Speed deviation with respect to time for extended SMIB without controller

From the above figure Fig 12 it can clearly seen that the speed deviation with respect to time is stable and this improves or enhances the stability of the power system with high settling time.

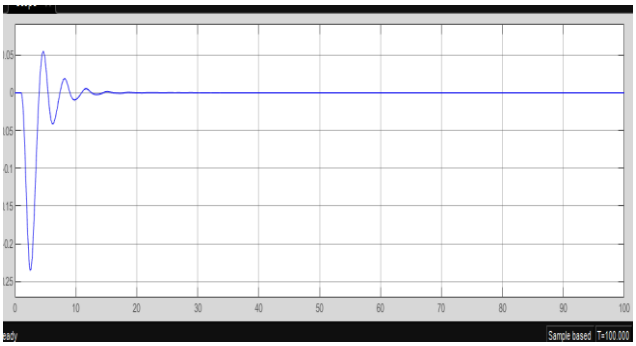

Fig. 13: speed deviation with respect to time for EXTENDED SMIB with PID controller

As we can see power system with Extended SMIB with PID controller in the above illustration, settling time was minimised along with in the limited speed deviation which inturn increases the power system stability with less settling time.

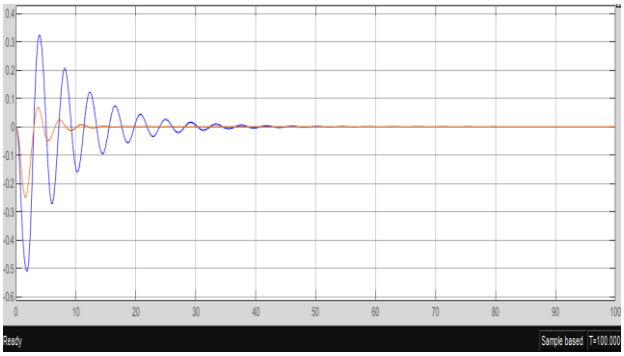

Fig. 14: comparision between EXTENDED SMIB with PID controler and with out PID controler

From the above illustration it can be clearly seen the comparision of Extended SMIB with and without PID controller, blue indicates more settling time and red indicates with less settling time using PID controller. It can be observed the greater reduction in settling time with reliability of power system.

V. Conclusion

Dual regulation of extended low head hydro power plant is achieved by controlling both wicket gate opening and runner blade position, which is connected to single machine infinite bus system. From the step responses it has been observed that the speed deviation for EXTENDED SMIB with and without PID. Results are obtained that the desired speed could be reached in a short time by using controllers.

Appendix

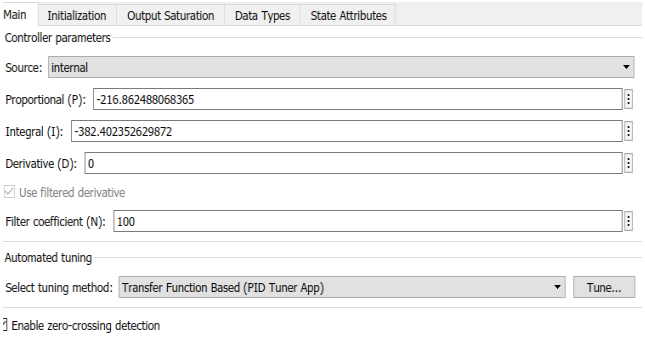

$T_a =$	**0.05**	K_A	**400**
$T_{gv} =$	**0.5**	$T_A , T_E ,$	**0.95, 0.05**
$V_t =$	**1.05**	$K_F =$	**0.025**
$\delta_0 =$	**65.1**	$T_F =$	**1.0**
$X_q =$	**0.57**	$X'_d =$	**0.360**
$G + jB =$	**0.248+j0.262**	R+jx=	**-0.34+ j0.926**
$X_d =$	**1.01**	D =	**0**
$T'_{do} =$	**7.6**	$V_{d0} =$	**1.34**
$(K_1$ to $K_6)=$	**0.55, 1.16, 0.66, 0.67, -0.99, 0.82**	$T_{rb} =$	**1.4**
$K_E =$	**1.010**	M =	**9.6**
$V_{q0} =$	**0.95**	ω_0	**377.17**

References

I. Amar President, O., Hocine Supervisor, L., & Nadia Examiner MCB, B. (2019). People's Democratic Republic of Algeria Ministry of Higher Education and Scientific Research THEME: Study of a Grid-Connected Photovoltaic System.

II. Bharatiraja, C., Kasilingam, G., Pasupuleti, J., Bharatiraja, C., & Adedayo, Y. (n.d.). Single Machine Connected Infinite Bus System Tuning Coordination Control using Biogeography-Based Optimization Algorithm. scindeks.ceon.rs.

III. Björk, J., & Johansson, K. (2019). Control Limitations due to Zero Dynamics in a Single-Machine Infinite Bus Network.

IV. Bux, R., Xiao, C., Hussain, A., & Wang, H. (2019, 11 16). Study of Single Machine Infinite Bus System with VSC Based Stabilizer. dl.acm.org, 159-163.

V. Chaib, H., Allaoui, T., Brahami, M., & Denai, M. (n.d.). Modelling, Simulation and Fuzzy Self-Tuning Control of D-STATCOM in a Single Machine Infinite Bus Power System.

VI. Chan, Z., & Aung, Z. (2020). Zar Ni Aung.

VII. Chen, J., & Engeda, A. (n.d.). IOP Conference Series: Earth and Environmental Science Design considerations for an ultra-low-head Kaplan turbine system Design considerations for an ultra-low-head Kaplan turbine system. iopscience.iop.org.

VIII. Czeslaw Banka, J. (2017). A RESEARCH PLAN FOR ASSESSING THE POWER AND ENERGY CAPABILITY OF A RIVER NETWORK UNDER AN INTEGRATED WIND/HYDRO-ELECTRIC DISPATCHABLE RÉGIME.

IX. Garbin, D. (2018). Analysis for the assessment of the wave energy and ISWEC productivity along the argentinian coast.

X. Ghosh, A., Das, A., & Sanyal, A. (2019, 10 1). Transient Stability Assessment of an Alternator Connected to Infinite Bus Through a Series Impedance Using State Space Model. Journal of The Institution of Engineers (India): Series B, 100(5), 509-513.

XI. GROULT, M. (2018). Optimization of Electromechanical Studies for the Connection of Hydro Generation MATHIEU GROULT KTH ROYAL INSTITUTE OF TECHNOLOGY SCHOOL OF ELECTRICAL ENGINEERING.

XII. Guo, B. (2019). Modelling and advanced controls of variable speed hydro-electric plants.

XIII. Haghighi, M., Mirghavami, S., Chini, S., energy, A.-R., & 2019, u. (n.d.). Developing a method to design and simulation of a very low head axial turbine with adjustable rotor blades. Elsevier.

XIV. Haghighi, M., Mirghavami, S., Ghorani, M., Energy, A.-R., & 2020, u. (n.d.). A numerical study on the performance of a superhydrophobic coated very low head (VLH) axial hydraulic turbine using entropy generation method. Elsevier.

XV. Houde, S., & Deschênes, C. (2019). Numerical investigation of flow in a runner of low-head bulb turbine and correlation with PIV and LDV measurements.

XVI. J French - US Patent 9, 8., & 2018, u. (2018). DIE K A N I K A N AT A UN.

XVII. Jacobsen, T. (2019). Distributed Renewable Generation and Power Flow Control to Improve Power Quality at Northern Senja, Norway.

XVIII. Kim, S. (2019, 9 17). Proportional-type non-linear excitation controller with power angle reference estimator for single-machine infinite-bus power system. IET Generation, Transmission and Distribution, 13(18), 4029-4036.

XIX. Komlanvi, A. (2018). Computer aided design of 3D of renewable energy platform for Togo's smart grid power system infrastructure Item Type Thesis.

XX. Machowski, J., Bialek, J., & Bumby, J. (2020). POWER SYSTEM DYNAMICS Stability and Control Second Edition.

XXI. Mashlakov, A. (2017). SIMULATION ON DISPERSED VOLTAGE CONTROL IN DISTRIBUTION NETWORK.

XXII. Masson, P., Weil, B., & Hatchuel, A. (2017). Design Theory.

XXIII. Mazhari, I. (2017). DC MICROGRID WITH CONTROLLABLE LOADS.

XXIV. Mukherjee, P., Das, A., & Bera, P. (2020). Design of P-I-D Power System Stabilizer Using Oppositional Krill Herd Algorithm for a Single Machine Infinite Bus System. In P. Mukherjee, A. Das, & P. Bera.

XXV. Naoe, N., on, A.-2., & 2019, u. (n.d.). A Three-Phase PM Generator with Double Rotors for Low-Head Hydropower–Trial Structure and Basic Characteristics. ieeexplore.ieee.org.

XXVI. Nichols, C. (2019). The Design of an In-Conduit Hydropower Plant with a Seal-Free Magnetic Transmission.

XXVII. Nygren, L., Ahola, J., & Ahonen, D. (2017). Programme in Electrical Engineering HYDRAULIC ENERGY HARVESTING WITH VARIABLE-SPEED-DRIVEN CENTRIFUGAL PUMP AS TURBINE.

XXVIII. Oo, M. (2019). Design of 50 kW Kaplan Turbine for Micro hydro Power Plant.

XXIX. Roca, W. (1675). MSc Dissertation Thesis MSc in Sustainable Energy Systems Modelling and Cost Analysis of a Hybrid Wind Turbine and Water Tower System as a Means of Energy Storage.

XXX. Ramana Rao KV, Nagendrababu, M., Valanginisarat, P., & Kallempudi Vahini. (2020). Implementation strategy to minimize the speckle noise from polarimetric sar data. International Journal of Mechanical and Production Engineering Research and Development, 10(3), 5455–5466. https://doi.org/10.24247/ijmperdjun2020520

XXXI. Salehghaffari, H. (n.d.). Hardware-In-The-Loop Vulnerability Analysis of a Single-Machine Infinite-Bus Power System.

XXXII. Shah, N., & Joshi, S. (2019, 3 1). Utilization of DFIG-based wind model for robust damping of the low frequency oscillations in a single SG connected to an infinite bus. International Transactions on Electrical Energy Systems, 29(3).

XXXIII. Shah, N., Electrical, S.-I., & 2019, u. (n.d.). Utilization of DFIG-based wind model for robust damping of the low frequency oscillations in a single SG connected to an infinite bus. Wiley Online Library.

XXXIV. Shahgholian, G., Hamidpour, H., & Movahedi, A. (2018). Transient Stability Promotion by FACTS Controller Based on Adaptive Inertia Weight Particle Swarm Optimization Method. advances.vsb.cz.

XXXV. Smil, V. (2019). Growth: from microorganisms to megacities.

XXXVI. Yang, W. (2017). Hydropower plants and power systems Dynamic processes and control for stable and efficient operation.

XXXVII. Ye, H., Pei, W., Kong, L., Power, T.-I., & 2018, u. (n.d.). Low-Order Response Modeling for Wind Farm-MTDC Participating in Primary Frequency Controls. ieeexplore.ieee.org.